

Edge preserving regularization for seismic traveltime tomography

Xiong Zhang*, Jie Zhang, University of Science and Technology of China (USTC)

Summary

We compare several regularization methods for traveltime tomography and present two improved methods for edge preserving regularizations. We could use a L2 norm of the model gradient or curvature as a part of the objective function to yield a smooth model solution, but the sharp edges of the model are often blurred. One way to generate a blocky model is to apply the L1 norm of the model gradient so that the model gradient is sparse. If we intend to preserve the sharp edges of the model and maintain smoothness elsewhere, then the edge preserving regularization with spatial variance is needed. We achieve that by introducing an edge preserving smoothing operator from seismic data processing to tomography. The improved methods for edge preserving regularization can make the model gradient sparser on the edge and decrease the impacts on the smoothness of non-edge area compared with the previous methods. We demonstrate the methods by testing with synthetics and real data.

Introduction

Geophysical imaging solutions are nonunique, imposed by the limited data information and limited model coverage. Therefore, model regularization is needed to obtain a high probability solution that exhibits with minimum structures required to fit data (Tikhonov and Arsenin, 1977). Such regularization includes uniform gradient smoothing or curvature smoothing expressed in terms of L2 norm (Zhang and Toksoz, 1998). Applying gradient smoothing allows linear variations in the model, while applying curvature smoothing allows nonlinear variation in the model.

L1 norm of model regularization is also applied to yield a blocky model in geophysics (Guitton, 2011; Elad, 2009; Loris et al., 2000; Schmidt, 2005). The merit of L2 norm is numerical stability and it is easy to implement, but it may generate a smooth solution with the sharp edge blurred. If we minimize the L1 norm of the model derivatives, we may get a blocky solution that the model gradient is sparse and the sharp edge of the model can be displayed clearly. However, it may also damage the smooth area of the model and it is difficult to calculate the derivatives of the object function than L2 norm (Schmidt, 2005). To overcome the difficulty of the L1 norm, some convex functions are presented to approximately solve the L1 norm problems such as the methods of hybrid norm and Huber norm (Claerbout, 2009; Li et al., 2010; Bube and Nemeth, 2007). The hybrid norm can change the L2 norm to L1 norm smoothly (Li et al., 2010), but it is unstable when the

hybrid norm approaches the L1 limit. In this study, we compare the regularizations including L1 norm, L2 norm and three edge preserving regularization methods.

The goal of an effective edge preserving regularization is to delineate sharp structure interfaces while suppressing the artifacts (Youzwishen and Sacchi, 2006; Namaki et al., 2011; Portniaguine and Zhdanov, 1999). In this study, we present two improved edge preserving regularization methods based on the previous method (Youzwishen and Sacchi, 2006) by borrowing the concept of edge preserving smoothing (EPS) operator (Luo et al., 2002; AlBinHassan et al., 2006). We compare the three edge preserving regularizations and analyze the strength and weakness of each method in 2D first-arrival traveltime tomography.

Theory

We first describe L1, L2 and the previous edge preserving regularization methods for traveltime tomography, and then present two improved edge preserving regularization methods. We fix L2 norm for data misfit while applying L1 or L2 norm for model regularization, thus, the general inversion object function can be written as

$$\varphi(m) = \|d_{obs} - G(m)\|_2^2 + \tau R(m) \quad (1)$$

Where m is model slowness; d_{obs} and $G(m)$ are the observed and calculated traveltimes. We apply wavefront ray-tracing technique to calculate both traveltimes and raypaths (Zhang and Toksoz, 1998) and apply conjugate gradients to solve a 2D traveltime tomography. The last term $R(m)$ denotes the regularization for the model and its form is mainly discussed in this study.

(1) L1 norm and L2 norm for the model derivative

We shall discuss the regularization by minimizing the first-order derivatives of the model. The two regularization methods can be written as:

$$\text{L1 norm: } R(m) = \sum_i |D_i m|, \quad (i = 1, 2) \quad (2)$$

$$\text{L2 norm: } R(m) = \|\nabla m\|^2 \quad (3)$$

Where $D_1 = \frac{\partial}{\partial x}$ and $D_2 = \frac{\partial}{\partial z}$ are derivative operators, and ∇ is the gradient operator. Minimizing the L1 norm of $D_i m$ ($i = 1, 2$) means that we want the matrix of $D_i m$ to be sparser than L2 norm. The slowness where $D_i m$ equals to zero remains constant, and the one where $D_i m$ equals to nonzero means slowness changing, the L1 norm solution is

Edge preserving regularization

thus blocky. For L1 norm, we use iteratively reweighting least squares (IRIS) method to approximately solve L1 norm problem. We may view the L1 norm as a (adaptively-weighted) version of squared L2 norm by setting a weighting matrix for the L2 norm to approximate the L1 norm (Elad, 2009).

(2) Edge preserving regularization

If we want to preserve sharp edges in the model solution, the matrix of the model derivative should be sparse on the edge of the velocity so that the velocity can be allowed to change abruptly on the edge. And we also want the non-edge area to be smooth, and we could modify the L2 norm of the model derivative to achieve that goal. For edge preserving regularization, different definition of the model edge may yield different edge preserving regularization method. If we define the area with large velocity gradient to be edges, the edge preserving regularization method by Youzwishen and Sacchi (2006) is expressed as following:

$$E1: R(m) = \sum_i \|W_i D_i m\|^2, \\ W_i = \text{diag} \left(\frac{1}{1+(D_i m_j)^2/c} \right), i = 1,2 \quad (4)$$

Where c is a positive constant which is small enough and it equals to a L2 norm if c is large enough. W_i is a weighting matrix; the weighting is inversely proportional to a function of the model gradient. We want the weighting close to zero on the edge of the model and to be one in other areas so that the smoothing is turned off on the edge but applied in non-edge area (Youzwishen and Sacchi, 2006). However, sometimes the contrasts of the weighting between the edge and non-edge areas are not large enough, and it may also damage the smoothness of the non-edge area if sharpening the edge. To overcome this difficulty, we can enhance the contrasts of the weighting between the edge and the non-edge area by introducing an operator to yield new methods.

To further enhance the model edge images, we borrow the concept of edge preserving smooth (EPS) operator (Luo et al., 2002; AlBinHassan et al., 2006) for sharpening seismic stack images for interpretation, but apply that for performing model regularization in tomography, and that yields a different edge preserving regularization method:

$$E2: R(m) = \sum_i \|W_i D_i m\|^2, \\ W_i = \text{diag} \left(\frac{1}{1+(D_i E(m_j))^2/c} \right), i = 1,2 \quad (5)$$

The function of EPS operator, $E(m_j)$, is for enhancing the model edge and smoothing the non-edge area in processing a seismic volume. If including the EPS operator, the weighting is more readily close to zero on the model edge

and one in non-edge area because the difference of the model gradient between the edge and the non-edge area becomes larger.

The regularizations (E1 and E2) may suffer from the problems to deal with the edge sometime as Figure (1b) shows because the weighting factor is also close to zero in non-edge area. And it violates our assumption that the weighting factor is one in non-edge area and zero on model edge. To overcome this difficulty, the model edge can be regarded as the area with large second derivatives of the model.

$$E3: R(m) = \sum_i \|W_i D_i m\|^2, \\ W_i = \text{diag} \left(\frac{1}{1+(D_i^2 E(m_j))^2/c} \right), i = 1,2 \quad (6)$$

D_i^2 is a second order derivative operator. Thus, the weighting parameter is close one in non-edge area in Figure (1b) because the second derivative of the model is zero in the non-edge area although the first order derivative is nonzero. The regularization method E3 also can deal with the case of Figure (1a). Note the only difference among E1, E2 and E3 is the weighting matrix.

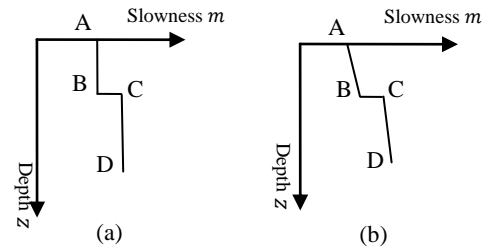


Figure 1 (a) For the segment AB and CD, the first order derivative $D_z m$ and the second order derivative $D_z^2 m$ are all zero. (b) For the segment AB and CD, the first order derivative $D_z m$ is not zero so it may be failed to make the weighting equal zero with first order derivative definition, but the second order derivative $D_z^2 m$ is zero.

Result comparisons

We show the results calculated with five regularization methods (Equation (2), (3), (4), (5), (6)) discussed in this study. We invert the velocity model as shown in Figures (2a & 3a) and the synthetic traveltimes are calculated from the model in Figures (2a & 3a). To compare the five regularization methods (Equation (2), (3), (4), (5), (6)), all the parameters are set to be nearly the same for different methods. The velocity model consists of 800*84 cells with a uniform spacing of 5 m. A total of 51 shots and 95 receivers for each shot are applied.

Edge preserving regularization

Figure 2 shows the results. The corresponding true model is layered with a constant velocity in each layer and the input initial model is a homogeneous model of 3000 m/s. The L2 norm of model derivative produces the smoothest model compared with the results of other regularization methods. We can tell the sharp boundary of the model from the result of L1 norm, but the velocity variation in other area shows step-like variation and it is not smooth, and this feature can be better observed if the true model contains velocity gradient. The edge preserving regularization methods (E1, E2 and E3) attempt to make the boundary sharp and make the velocity variation in other area like L2 norm. We choose the same threshold value c (balancing the L2 norm and the edge preserving regularization) for the three edge preserving regularizations; Figures (2d, 2e and 2f) show method E2 and E3 can yield the result with sharper edge than E1 method does, because the EPS operator can help to produce sharp boundary and

smooth the non-edge area and the weighting matrix can be more reasonable.

Figure 3 shows the results with which the corresponding true model is layered with a velocity gradient in the top layer and the input initial model is a homogeneous model of 3800 m/s. The L2 norm can yield a robust model with the accurate velocity gradient in the top layer but the sharp edge is blurred. The L1 norm can present the sharp edge but the step-like structure in the top layer is much clearer than what the Figure 2c shows because of the velocity gradient of the true model. In Figure 3 the threshold value c is also the same for the three edge preserving regularization methods. The top of the edge in Figure 3f is the sharpest of the three edge preserving regularization methods. The edge preserving regularization method E3 can not only present the sharp edge but also the velocity gradient can be preserved.

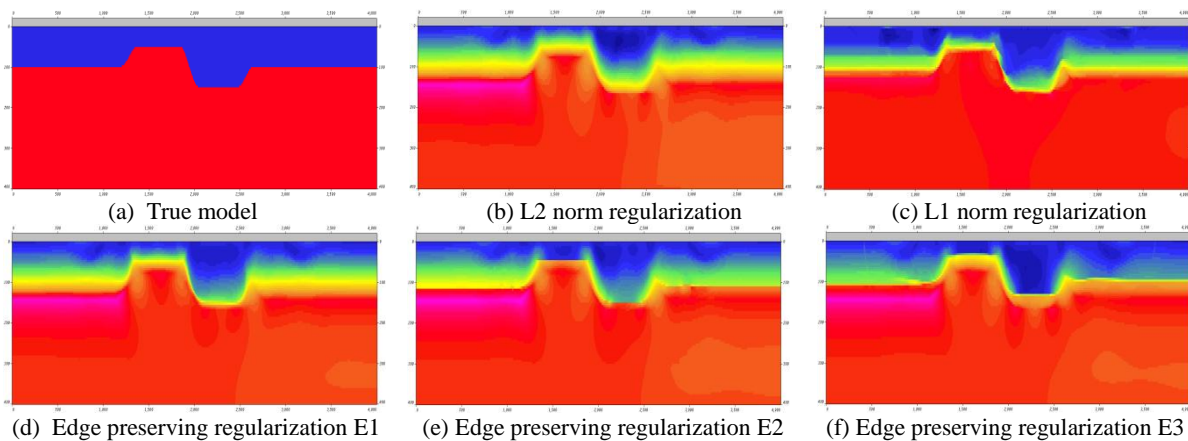


Figure 2 The synthetic data example calculated with five model regularization methods (Equation (2), (3), (4), (5), (6)).

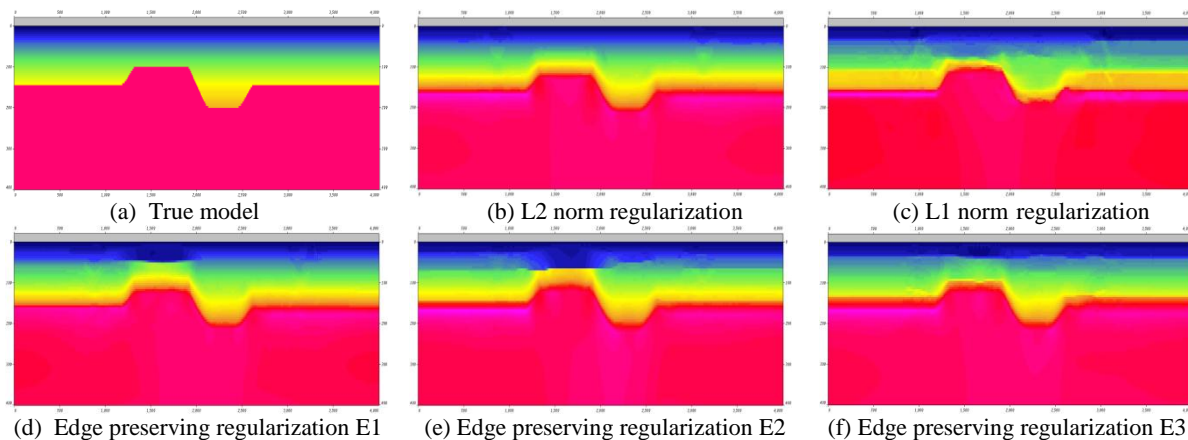


Figure 3 The synthetic data example calculated with five model regularization methods (Equation (2), (3), (4), (5), (6)).

Edge preserving regularization

Field data example

The regularization methods discussed in this study have been applied in the field data. We conducted the tomography studies with a model consisting of 6788*204 cells with a uniform grid spacing of 5.0 m. To obtain an initial model for the traveltimes tomography, we first conducted the delay-time method to get the initial model for GLI method, and then applied the GLI method to yield the initial model that Figure 4a shows. The result of GLI method shows that the velocity variation among the three layers of the initial model is distinct especially in the first layer. Figure 4 shows the L2 norm regularization yield the smoothest result; it is easy to bring in abruptly velocity variation for L1 norm; the edge preserving regularizations can yield models with sharp boundary. The high-velocity bodies in the second layer between the initial model and the other models are different because we assumed a three-layer model for the GLI method. The traveltimes tomography can correct the high-velocity part of the initial model. The boundary of the first layer in Figures (4e & 4f) is shallower than the one of Figure 4d although the boundary of the second layer in Figure 4d is blurred. If we start the edge preserving regularization from the second iteration for the method E1, we can see easily that it is harder to reveal the boundary for method E1 than the other edge preserving regularizations.

Conclusions

We have discussed the characteristics of L1 norm, L2 norm and edge preserving regularizations. To enhance the model edge and preserve the characteristics of L2 norm we presented two modified edge preserving regularization methods. The L2 norm can yield a smooth solution but blur the details of the model. L1 norm can reveal the details but it can produce some artifacts of step-alike structure. The improved edge preserving regularization can not only reveal the details on the model edge but also make the non-edge area like the L2 norm solution, because it focuses on the sparseness of the edge with strong velocity variation. We introduced the EPS operator to sharpen the edge and smooth non-edge area of the model because it is helpful for constructing the weighting matrix. The new edge preserving regularization methods can make the edge sharper with the same parameter setting and decrease the impacts on the smoothness of the non-edge area.

Acknowledgement

We appreciate the support from GeoTomo, allowing us to use TomoPlus software package.

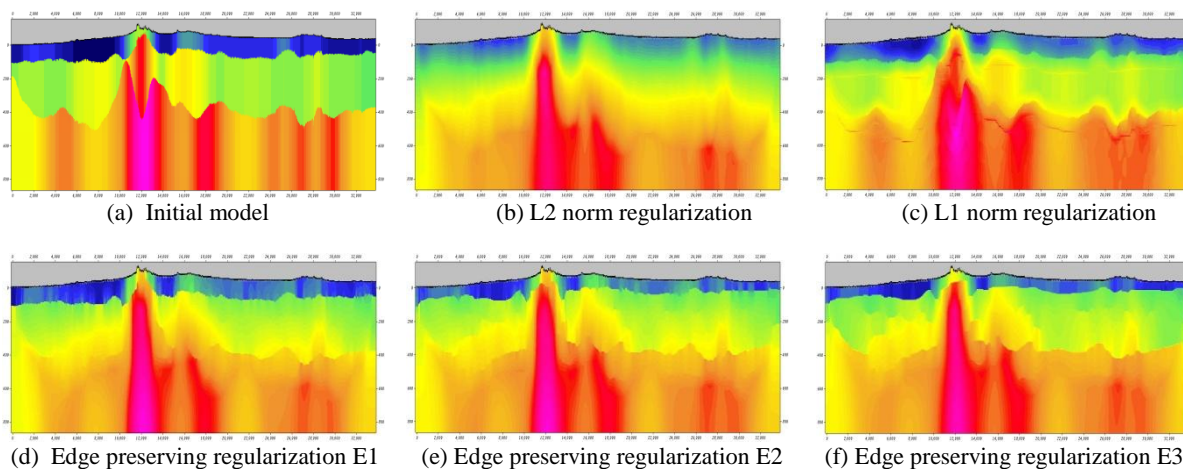


Figure 4 The field data example calculated with five model regularization methods (Equation (2), (3), (4), (5), (6)). The starting model is as (a) shows.

EDITED REFERENCES

Note: This reference list is a copy-edited version of the reference list submitted by the author. Reference lists for the 2012 SEG Technical Program Expanded Abstracts have been copy edited so that references provided with the online metadata for each paper will achieve a high degree of linking to cited sources that appear on the Web.

REFERENCES

- Al Bin Hassan, N. M., Y. Luo, and M. N. Al-Faraj, 2006, 3D edge-preserving smoothing and applications: *Geophysics*, **71**, no. 4, A13–A17.
- Bube, K. P., and T. Nemeth, 2007, Fast line searches for hybrid L1/L2 norm and Huber norms: *Geophysics*, **72**, no. 2, 5–11.
- Claerbout, J. F., 2009, Blocky models via the L1/L2 hybrid norm: SEP Report, **139**, 1–10.
- Elad, M., 2009, Sparse and redundant representations: From theory to applications in signal and image processing: Springer Science+Business Media, Google e-book.
- Guittou, A., 2011, A blocky regularization scheme for full waveform inversion: 81st Annual International Meeting, SEG, Expanded Abstracts, 2418–2422.
- Li, Y., Y. Zhang, and J. Claerbout, 2010, Geophysical applications of a novel and robust L1 solver: 80th Annual International Meeting, SEG, Expanded Abstracts, 3519–3523.
- Loris, I., G. Nolet, I. Daubechies, and F. A. Dahlen, 2000, Tomographic inversion using L1-norm regularization of wavelet coefficients: *Geophysical Journal International*, **170**, 1–14.
- Luo, Y., M. Marhoon, S. A. Dossary, and M. Alfaraj, 2002, Edge-preserving smoothing and applications: *The Leading Edge*, **21**, 136–141.
- Namaki, L., A. Gholami, and M. A. Hafizi, 2011, Edge-preserved 2-D inversion of magnetic data: an application to the Makran arc-trench complex: *Geophysical Journal International*, **184**, 1058–1068.
- Portniaguine, O., and M. S. Zhdanov, 1999, Focusing geophysical inversion images: *Geophysics*, **64**, 874–887.
- Schmidt, M., 2005, Least squares optimization with L1-norm regularization: Technical Report.
- Tikhonov, A. N., and V. Y. Arsenin, 1977, Solutions of ill-posed problems: W. H. Winston and Sons.
- Youzwishen, C. F., and M. D. Sacchi, 2006 Edge preserving imaging: *Journal of Seismic Exploration*, **15**, 45–58.
- Zhang, J., and M. N. Toksoz, 1998, Nonlinear refraction travelttime tomography: *Geophysics*, **63**, 1726–1737.